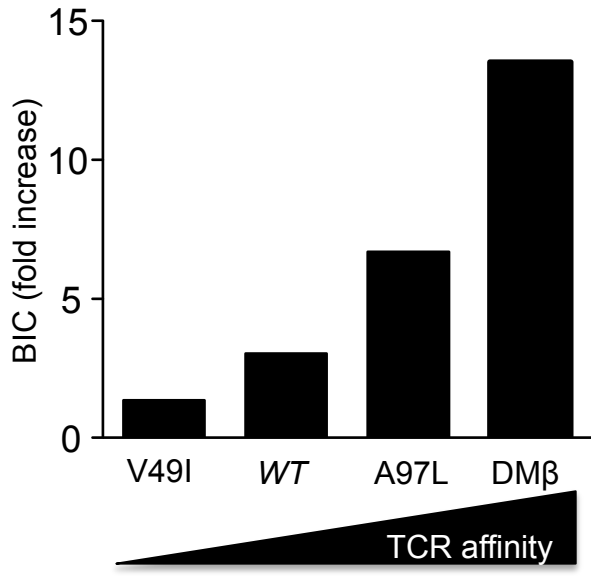
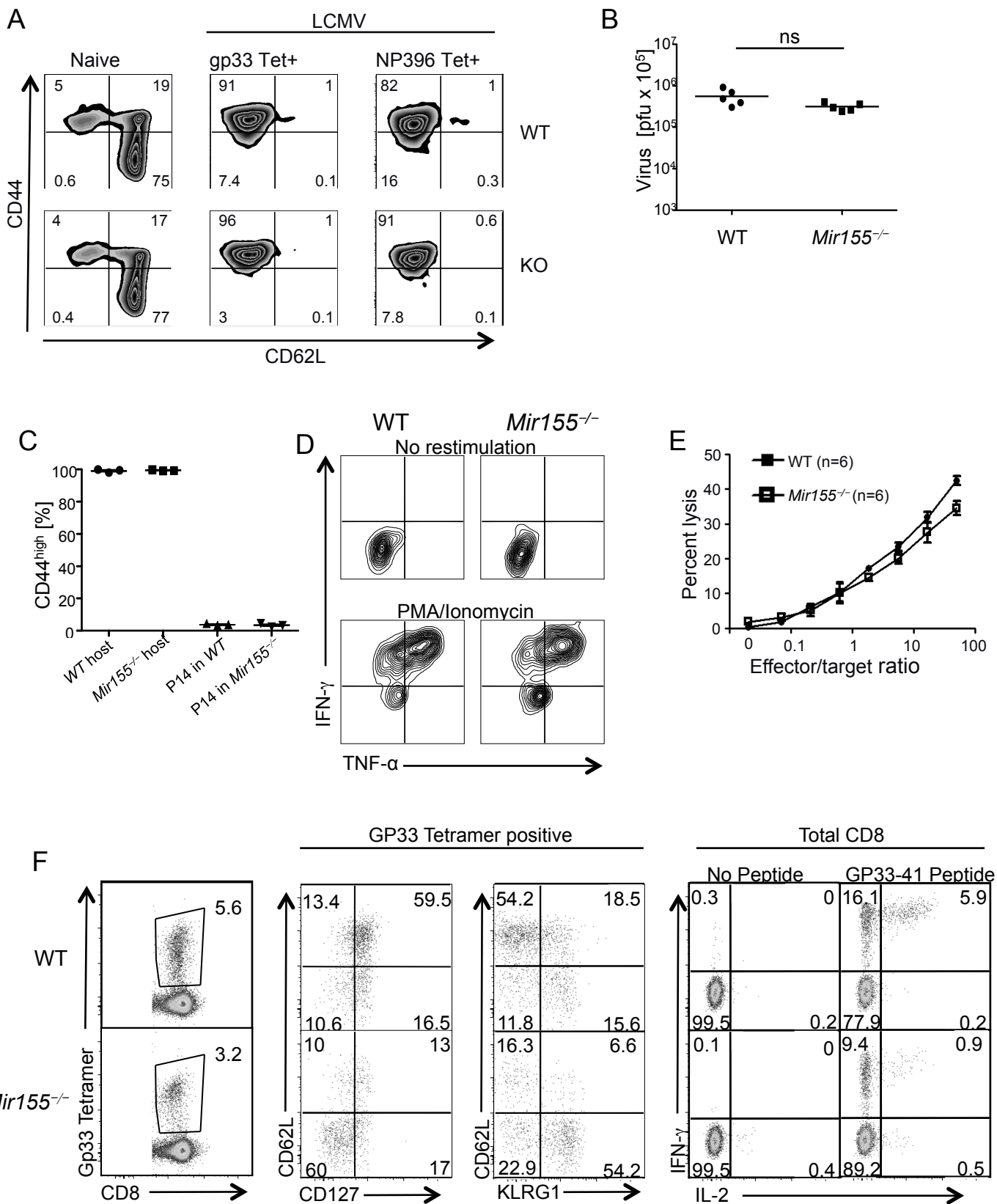


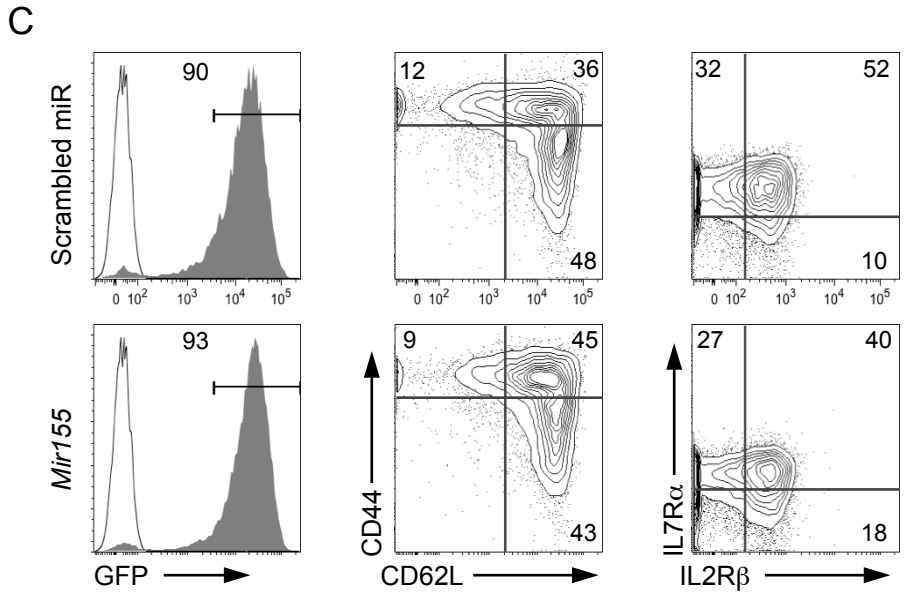
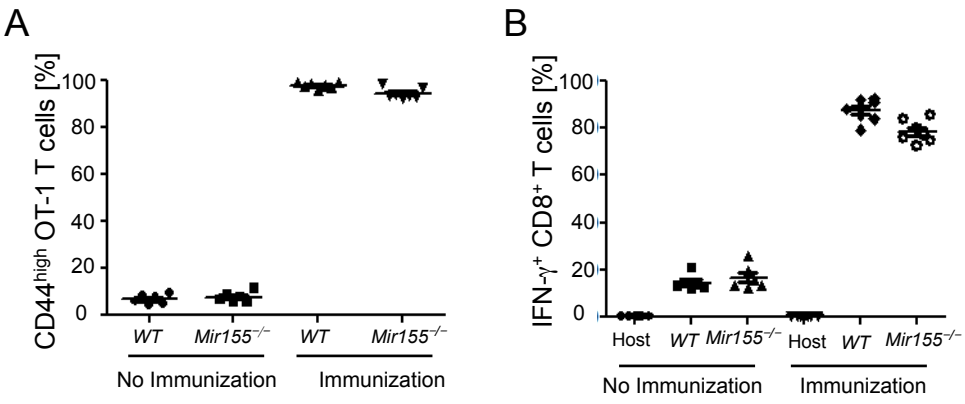
Supplemental Figure 1 related to Figure 1A



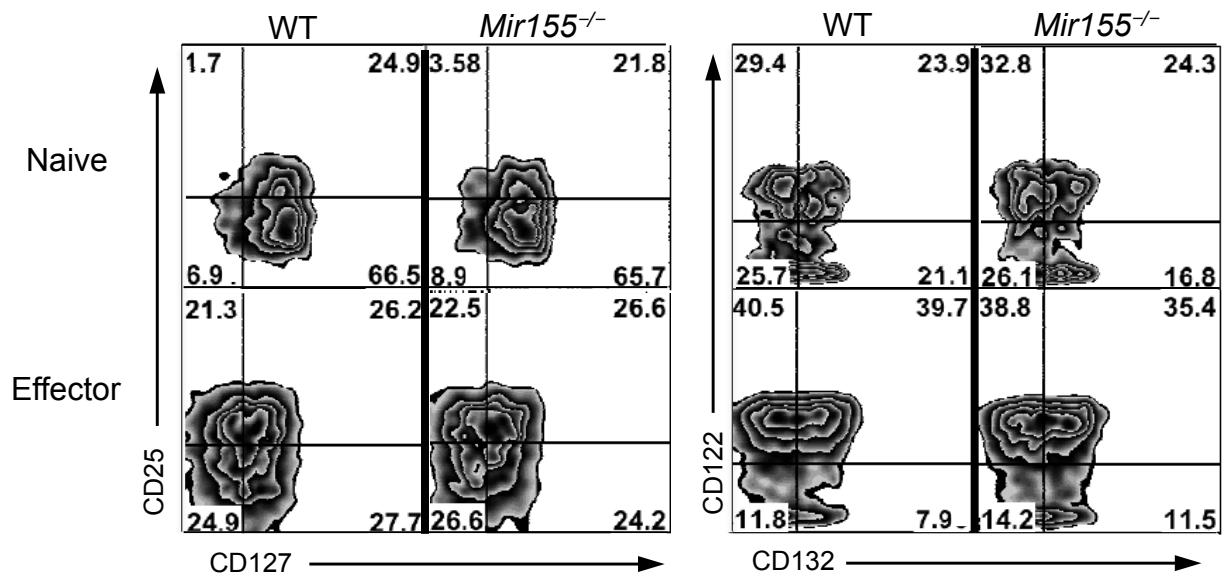
Supplemental Figure 2 related to Figure 2 A-C



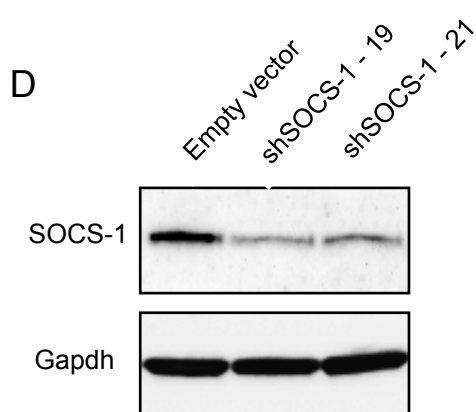
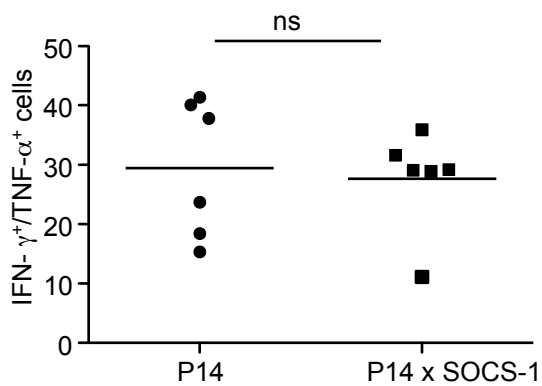
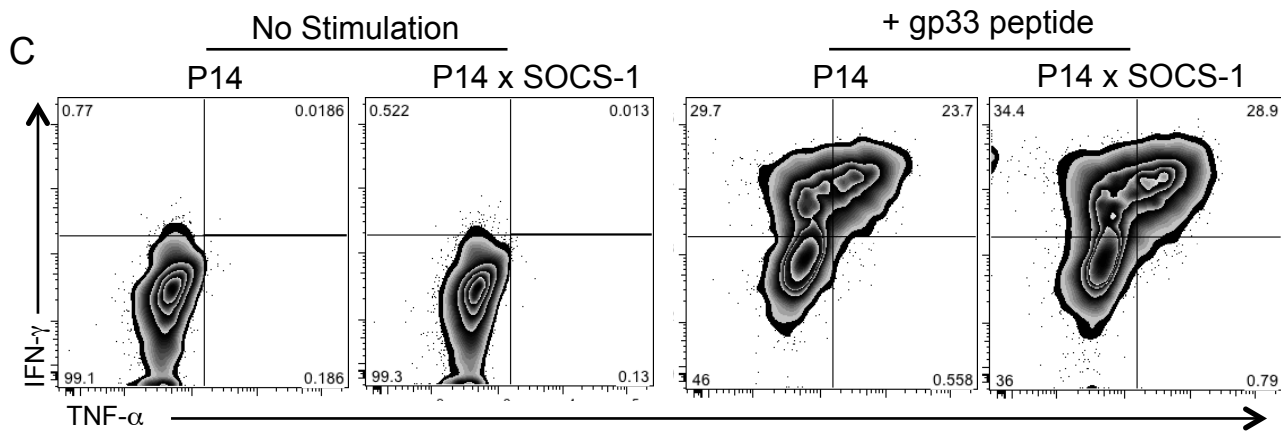
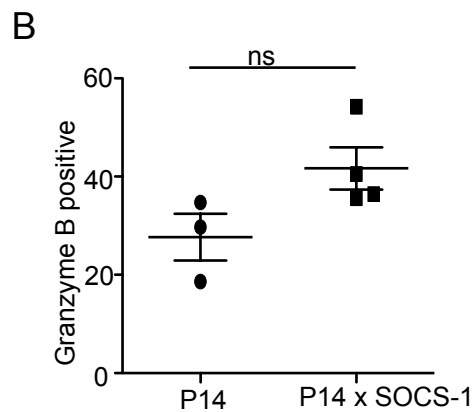
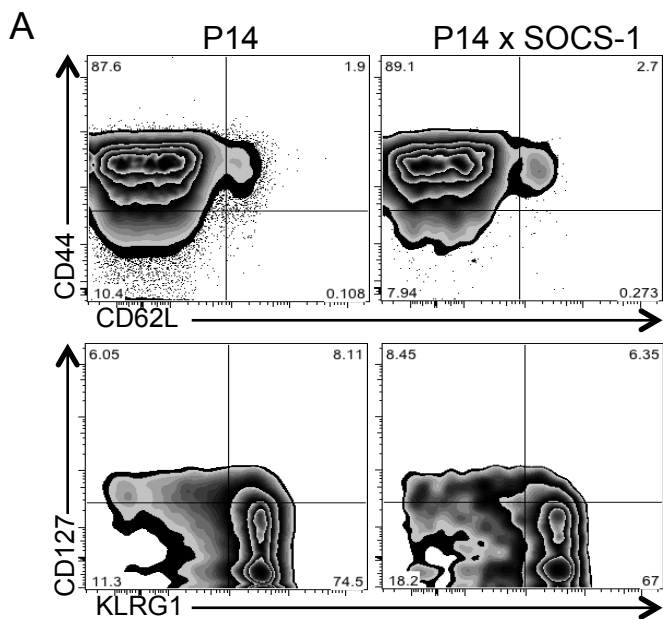
Supplemental Figure 3 related to Figure 5



Supplemental Figure 4 related to Figure 6



Supplemental Figure 5 related to Figure 7



Legends to supplementary figures

Supplemental Figure 1, related to Figure 1: Early expression of BIC is dependent on TCR affinity. Expression fold-changes (0-6h) in the levels of BIC (pre-miR-155) non-coding RNA in the panel of primary human CD8⁺ T cells transduced with NY-ESO-1-specific TCRs of increasing affinity following TCR stimulation with NY-ESO-1₁₅₇₋₁₆₅ multimers. Data are from one microarray experiment.

Supplemental Figure 2 related to Figure 2: miR-155 independent acquisition of effector functions but defective memory formation. (A) Differentiation markers on naïve, or gp33 and np396 tetramer positive, virus specific CD8⁺ T cells from blood of naïve or day 8 LCMV WE infected wild type (WT) and *Mir155*^{-/-} mice were measured by flow cytometry. (B) Virus titers were determined in spleens at day 5 of infection. (C) Lack of virus persistence was confirmed by transferring naïve P14 T cells into mice on day 21 after LCMV infection. Pictured is CD44 expression of gp33-tetramer⁺ host and donor P14 cells at 3 days after the transfer. (D) Production of indicated cytokines from gp33 tetramer⁺CD8⁺ splenocytes after *in vitro* restimulation with PMA/Ionomycin at day 8 post infection. (E) Cytotoxic activity of gp33 tetramer⁺CD8⁺ T cells at day 8 after LCMV infection was determined by chromium release assay using peptide-pulsed target cells. Representative results from one out of two experiments are shown. (F) Phenotype and cytokine production (upon peptide restimulation) of splenic LCMV specific, gp33 tetramer⁺CD8⁺ T cells from infected wild type (WT) and *Mir155*^{-/-} mice was monitored 3 month upon infection. Points are representing single mice and the line is the mean (B, C). Representative results of one out of three independent experiments with three to five mice are pictured.

Supplemental Figure 3, related to Figure 5: Acquisition of effector phenotype and IFN- γ production upon vaccination is independent of miR-155. Wild type (WT) and *Mir155*^{-/-} OT-1 cells were transferred into WT mice before vaccination. (A) Upregulation of CD44 as well as (B) IFN- γ production by respective OT-1 cells was measured in draining lymph nodes on day 4 after vaccination upon restimulation. Data are from one representative out of two experiments with three to five mice per group. (C) GFP marker positive scrambled miR control and miR-155 transduced cells were stained for the indicated activation markers and cytokine receptors before injection into tumor bearing mice.

Supplemental Figure 4, related to Figure 6: miR-155 does not affect cytokine receptor expression in naïve CD8⁺ T cells. Naïve (CD44^{low}CD62L^{high}) CD8⁺ T cells from untreated wild type (WT) or *Mir155*^{-/-} mice were stained for indicated cytokine receptors. Representative results from one out of two experiments with three to five mice are shown.

Supplemental Figure 5, related to Figure 7: Elevated SOCS-1 expression does not affect CD8⁺ effector phenotype. Downregulation of SOCS-1 by retroviral shSOCS-1 transduction. P14 and P14xSOCS-1 transgenic T cells were transferred into wild type mice before infection with LCMV WE. Expression of (A) activation markers on day 8 and (B) Granzyme B on day 7 was monitored on P14 cells from spleen and displayed as mean +/- SEM. (C) Cytokine production of splenic P14 T cells was measured upon *in vitro* stimulation with gp33 peptide. Representative data from one out of two experiments (N= 3 to 4) are pictured and the line in the last panel represents the mean. (D) Inhibition of SOCS-1 expression by two different shSOCS-1 constructs was validated by Immunoblot on transduced T cells. shSOCS-1-21 was used for rescue of pSTAT5 generation in *Mir155*^{-/-} cells (Figure 6D).